

Field Techniques Manual: GIS, GPS and Remote Sensing

- Section C: Techniques

Chapter 8: Image Interpretation and
Processing

8 Image Interpretation and Processing

This chapter examines the two main approaches that we can use to add geographical information to a fieldwork-based survey: manual interpretation and automatic feature classification. The first to be considered is the manual delineation of features using image interpretation and conventional cartographic techniques. That is followed by a brief explanation of digital image processing techniques that can use variations in the spectral response of features to produce computer-generated maps.

8.1 Image interpretation

The features that our brains use when we interpret an image can be grouped into six main types, summarised below and in Figure 8-1:

1. **Tone:** variations in relative brightness or colour.
2. **Texture:** areas of an image with varying degrees of ‘smoothness’ or ‘roughness’.
3. **Pattern:** the arrangement of different tones and textures; may indicate certain types of geology or land use.
4. **Shape:** distinct patterns may be due to natural landforms or human shaping of the land.
5. **Size:** recognition of familiar objects allows size estimation of other features; size is an important aspect of association: for instance, a 20 km-wide circular surface depression is unlikely to be a sinkhole, but might be a volcanic caldera.
6. **Association:** the context of features in an image, e.g. a drainage pattern.

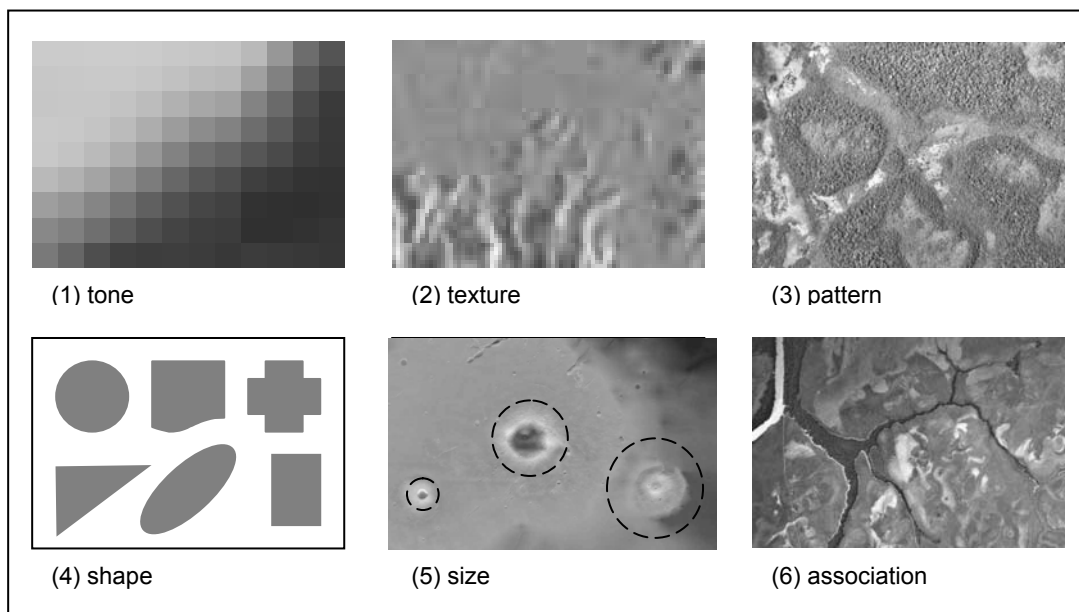


Figure 8-1 Features used in image interpretation.

Tone, texture, pattern and shape are all influenced by illumination conditions and vegetation cover: they can therefore vary with time. Subtle features, such as buried archaeological structures, are best detected with the low sun angles and long shadows found at the start and end of the day, as well as during the winter season. Conversely, when mapping rugged terrain, try to use mid-day or summer imagery to reduce the loss of detail caused by valley-side shadows. Wet season and dry season variations in vegetation cover may be linked to variations in hydrogeology. The orientation, size and density of shadows can give clues about an area's relief and degree of dissection, as illustrated in Figure 8-2.



The following features can be identified:

- *lava flows*: recent flows have the darkest tone; the oldest flow has a grey tone and the most fragmented texture (top right)
- *volcanic cones and craters*: discrete circular shapes and tonal contrasts with surrounding terrain
- *a geological fault zone*, possibly part of a fissure volcano (bottom left)

Figure 8-2 Interpretation of an airphoto from volcanic terrain.

8.1.1 Drainage patterns

The patterns produced by drainage networks are a useful guide to underlying soils and geology, as illustrated in Figure 8-3 and the subsequent summary table.

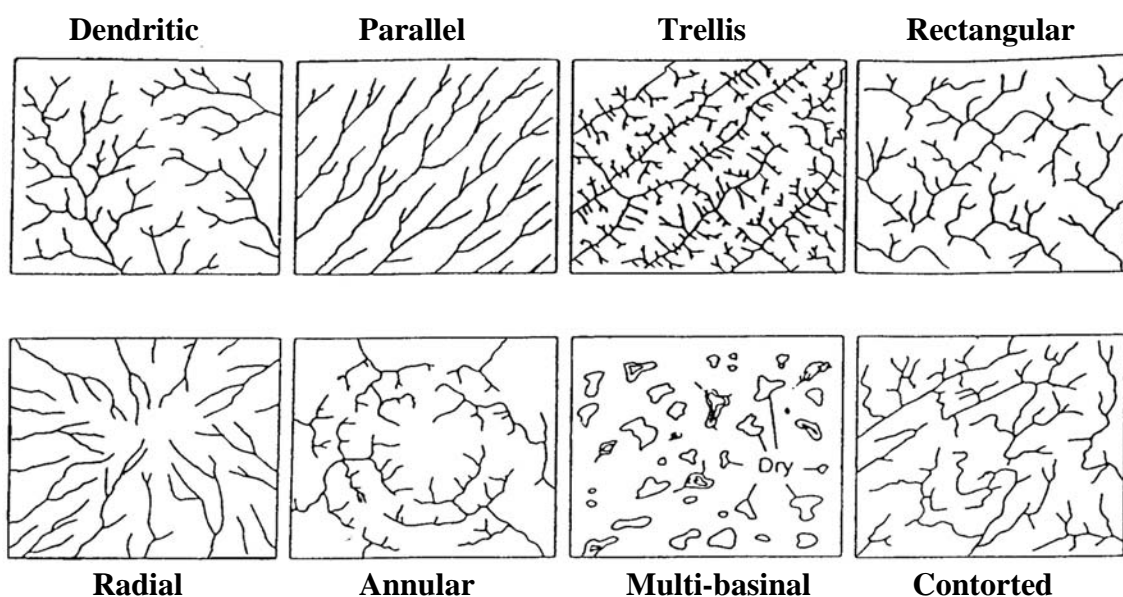


Figure 8-3 Common drainage patterns and their interpretation (after Howard 1967).

Pattern	Interpretation
Dendritic	Horizontal sediments or uniformly resistant crystalline rocks. Gentle regional slope at time of drainage inception.
Parallel	Moderate to steep slopes but also found in areas of parallel, elongate landforms.
Trellis	Dipping or folded sedimentary, volcanic, or low-grade metasedimentary rocks; areas of parallel fractures, exposed lake or seafloors with beach ridges
Rectangular	Joints and/or faults/fractures at right-angles. Lacks orderly repetitive quality of trellis pattern: streams and divides lack regional continuity.
Radial	Volcanoes, domes, and residual hills/inselbergs. A complex of radial patterns in a volcanic field might be called multi-radial.
Annular	Structural domes and basins, diatremes and possibly igneous stocks
Multi-basinal	Hummocky surface deposits; differentially scoured bedrock; areas of recent volcanism, limestone solution, and/or permafrost.
Contorted	Coarsely layered metamorphic rocks. Dikes, veins, and migmatized bands provide the resistant layers in some areas.

The most common drainage pattern is *Dendritic*, typical of relatively uniform, moderately well-drained soils and rocks: a variant pattern; and *Pinnate*, forms in easily-erodible silty deposits, such as wind-blown glacial loess. Dry valleys and sink-holes dominate in limestone landscapes, with most of the water flowing through cave systems, producing a *Dislocated* drainage pattern. Formerly glaciated terrain may have a *Deranged* drainage pattern, due to the melting of ice blocks within the glacial till, producing ‘kettle-hole’ lakes and a landscape with a poorly developed drainage network. Most of the other drainage patterns are strongly influenced by geological structures, such as alternate beds of gently-dipping soft and hard sedimentary rocks (e.g. *Trellis*); bedding and joint structures in metamorphic rocks or hard sandstones (*Rectangular*); joint structures in plutonic rock masses, such as granite (*Annular*); fault zones (*Elongate*, *Parallel*) and volcanoes (*Radial*). Detailed reviews of drainage pattern and image interpretation are given in Avery & Berlin (1992), Lawrance *et al* (1993) and Drury (2001).

Drainage texture or drainage density (the total length of channel in a given square kilometre) is a good indicator of the permeability of the soil and rock of the study area. Highly permeable substrates, such as limestone bedrock or sandy soils, have a low drainage density, as most of the surface water ends up underground. Conversely, relatively impermeable clay-rich soils and soft rocks such as shale or mudstone may have very high drainage densities, due to extensive overland flow and severe gully erosion. This produces highly dissected landscapes known as ‘badlands’ because of their unsuitability for farming. River rejuvenation or tectonic uplift can trigger headward fluvial erosion and enhanced gullying, leading to a higher drainage density.

8.2 Geomorphological mapping

The interaction between Earth-surface processes (i.e. weathering, erosion, deposition) and a few sub-surface processes (notably surface movements caused by earthquakes) tends to produce distinctive sets of landforms made up of distinctive materials. Examples are fluvial processes producing terraces made up of alluvium or sub-glacial processes forming

drumlins made of boulder clay. Thus from our knowledge of geomorphology we can make a fair estimate of the formative processes and component materials of a given landform (Figure 8-4). This can be very useful in hazard assessment, as landforms may provide clues to the types of hazardous processes occurring in the study area, as well as the frequency and magnitude of hazardous events. Similarly, landforms may also give useful indications of earth resources, notably various sizes of aggregate associated with coastal, fluvial and fluvio-glacial deposits.

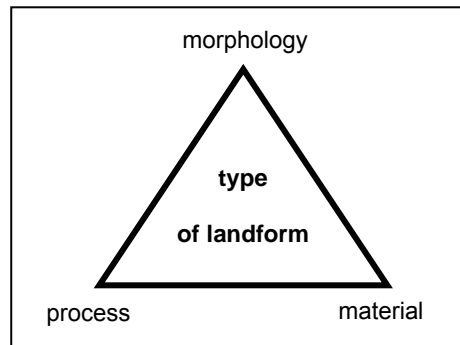


Figure 8-4 The 'Holy Trinity' of geomorphology: process, material and morphology.

Geomorphological mapping is based on the identification of landforms or assemblages of landforms. This involves subjective assessment by the mapper, with the most reliable maps being produced by the most experienced geomorphologists (e.g., Brunsten *et al* 1975; Cooke & Doornkamp 1990; Fookes 1997). The best type of remote sensing data for detailed geomorphological mapping is vertical aerial photography, because of the general high degree of detail and possible stereoscopic (3-D) viewing. Image interpretation and fieldwork are iterative tasks: preliminary satellite or airphoto mapping precedes the initial field reconnaissance survey, with each stage of field survey producing additions or corrections to the image interpretation scheme.

Some satellite data, notably SPOT and IKONOS panchromatic imagery (with 3 m and 1 m pixels respectively), can be viewed and interpreted stereoscopically. Digital Elevation Models (DEMs) can be generated from the SPOT and IKONOS data, allowing geomorphological mapping, 3-D visualisation and 'virtual reality' fly-overs of study areas. The only down-side of the SPOT and IKONOS imagery is its relatively high cost. However, for c. £60 the ASTER sensor can provide a DEM covering 60 km x 60 km with 15 m pixels and 15 m contours, equivalent to a 1:50,000-scale map. For regional-scale studies, free 1:250,000 DEM data are available from the Shuttle Radar Topography Mission (SRTM).

One way to reduce to subjective/interpretive element is to limit a survey to *morphological mapping*: breaks of slope, amounts of slope and directions of slope are mapped using airphoto stereoscopy, but no attempt is made to interpret the origin and composition of mapped features. Taking things a step further, *morphometric mapping* relies entirely on the field mapping of slope breaks, steepness and aspect. Although this produces a map with a high degree of objectivity (and replicability), such 'walk-over' surveys take far longer than airphoto interpretation.

8.3 Mapping geo-ecological features

Geo-ecological mapping has been developed since the 1940s, when initial interest focused on using aerial photography to map the suitability of terrain for military purposes. By the 1950s, the Land Systems methodology had been developed to map vast areas of Australia and assess their suitability for agriculture (Christian and Stewart 1952). The different textures, tones and patterns displayed by different vegetation types are utilised in Land Systems mapping to map geo-ecological zones, each with a distinctive type of vegetation cover, soil, geology and hydrology. This process of ‘mapping by proxy’ allows large tracts to be mapped from remotely sensed images with just a few visits to check the ‘ground-truth’ at representative sites. The case studies feature an example of Land Systems mapping along the Luangwa River, Zambia, based on the interpretation of Landsat imagery and aerial photography (Figure 8-5). A number of other mapping systems are based on identifying geo-ecological features, notably that of the ITC (Verstappen & Van Zuidam 1975; Meijerink 1988) and Brunsdon *et al*'s (1975) rapid geomorphological mapping techniques for civil engineering projects. Methods of aerial mapping and monitoring, from an ecological perspective, are reviewed by Clarke (1986).

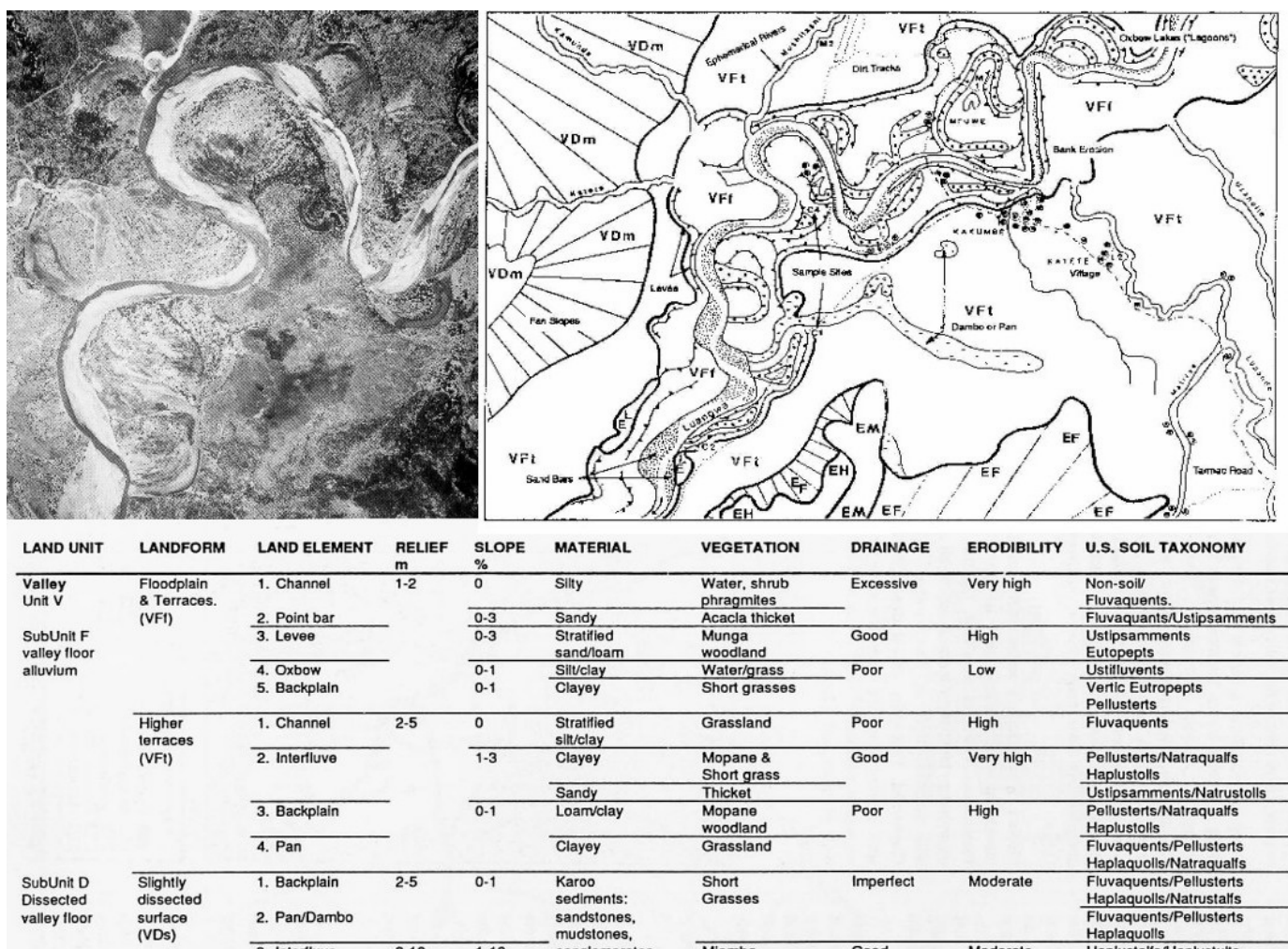


Figure 8-5 Extract from a Land Systems map and classification system, derived from 1:40,000 aerial photography (inset): Luangwa Valley, Zambia (Teeuw 1990).

A brief summary of geo-ecological features that can be detected by remote sensing is given in Table 8-1.

Table 8-1 Summary of geo-ecological remote sensing applications (NIR, MIR and TIR are near, middle and thermal infra-red). Black = very useful, grey = may be useful, blank = not useful. See Figure 5.1 for the spectral ranges of NIR, MIR and TIR (after Leuven et al. 2000).

Water	AIRBORNE (cm to m detail)						SATELLITE (m to km detail)				
	visible	lidar	NIR	MIR	TIR	radar	visible	NIR	MIR	TIR	Radar
Aquatic plants			Black								
Bathymetry		Black	Grey			Grey					
Flood extent					Black	Black				Black	Black
Ice cover		Black									
Pollution: - oil											
- chemical											
Temperature											
Turbidity: - algae			Black	Grey					Black	Grey	
- plankton			Black								
Landscape	visible	lidar	NIR	MIR	TIR	radar	visible	NIR	MIR	TIR	Radar
Animal counts	Black				Black						
Archaeology	Grey					Grey		Black			Grey
Channel changes							Grey	Grey			
Drainage pattern									Black		Black
Dykes / walls	Grey		Grey				Grey	Grey			
Floodplain	Grey						Grey	Black		Grey	Black
Land: - built-on							Grey	Black			Grey
- contaminated	Grey			Grey	Black		Grey	Grey	Grey	Grey	
Relief											
- surface change							Grey				Black
- mm subsidence											
Rock or soil type	Grey			Black	Grey	Grey	Grey		Black	Grey	Grey
Soil moisture											Black
Soil / sed texture		Black		Grey					Grey		
Snow / ice cover	Grey		Grey		Grey		Grey	Grey		Grey	
Seepage / spring	Grey		Black		Black	Grey		Black		Black	Grey
Vegetation - type											
- woody biomass	Grey	Black	Grey				Grey	Grey			Black
- height	Grey		Grey								
- stress	Grey		Black				Grey	Black			
	visible	lidar	NIR	MIR	TIR	radar	visible	NIR	MIR	TIR	Radar

8.4 Human population estimates

Population numbers and population densities are essential data for planners both in urban and rural settings. Comparison with earlier records allows an assessment of increasing or

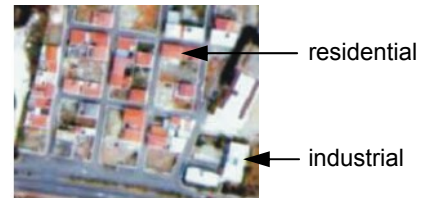
decreasing population trends. Areas suitable for development can be identified, along with areas that are already over-crowded. In civil emergency planning, airphotos are an effective way of identifying vulnerable populations, as well as evacuation routes. In many developing countries, airphotos may offer the best means of gaining population information (Figure 8-6).

Figure 8-6 How aerial photography can be used in estimating urban population densities.

1. Delimit homogenous housing area
2. Calculate area
3. Determine the number of buildings
4. Determine number of storeys/building

Built-up area = 1.1 ha
 Number of buildings = 24.5
 Number of flats/storey = 2
 Average number of storeys = 2
 Average family size = 5

$5 \times 2 \times 2 = 20$ people/building
 $20 \text{ people} \times 24.5 \text{ buildings} = 490 \text{ people}$
 $490 / 1.1 = 445 \text{ people / hectare}$



8.5 Digital image processing

Scanned images are made up of Digital Numbers (DNs): the lower the DN values, the darker the resulting greyscale image, as illustrated in Figure 8-7.

2050	2044	2047	2061	2076	2087
2060	2059	2057	2060	2067	2074
2073	2070	2066	2064	2065	2070
2085	2084	2078	2073	2072	2073
2097	2098	2094	2088	2085	2084
2110	2113	2110	2105	2101	2100
2122	2127	2127	2122	2119	2118
2133	2140	2142	2139	2137	2137
2142	2151	2155	2155	2155	2156
2148	2158	2165	2168	2170	2173
2149	2160	2170	2176	2181	2187
2147	2159	2170	2180	2189	2198
2141	2154	2167	2180	2192	2205
2133	2147	2161	2176	2192	2207
2123	2137	2153	2169	2186	2203
2114	2128	2145	2162	2180	2198

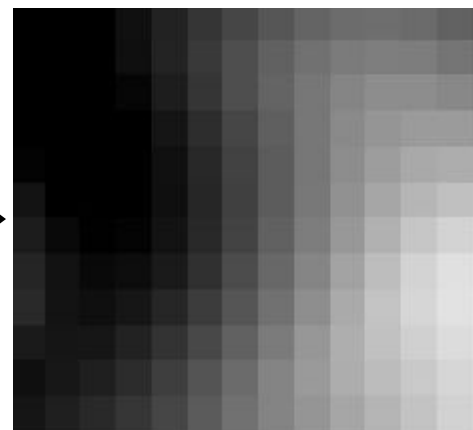


Figure 8-7 An example of DN values in a raster matrix, forming the greyscale image on the right.

Digital images have some major advantages over paper or film (analogue) images: they take up less storage space, perfect copies can be created time and time again, they can be reduced or enlarged at the push of a button, cartographic errors can easily be removed, and - most important of all - digital images can be processed using statistics, to enhance, analyse and classify their features. There are three main stages in the digital image

processing of remotely sensed data: pre-processing, removing distortions from the imagery; image enhancement, highlighting features in the imagery; and image classification, producing maps of the features in the imagery.

8.5.1 Pre-processing

Distortions are inherent in remotely sensed imagery, whether from satellite or airborne platforms. Dust and water vapour in the atmosphere will absorb and reflect certain wavelengths of electromagnetic radiation, especially at shorter wavelengths and particularly in the blue part of the spectrum. Such *atmospheric distortions*, or attenuation, can be corrected by the ‘black body’ approach: clear water absorbs near infra-red and middle infra-red radiation, so its DN values in those wavelengths should be at or close to zero. If, say, the DN values for a middle infra-red band over water range from 18 to 27, then 18 could be subtracted from all of the DN values forming the raster matrix for that band, giving features over water ‘truer’ DN values ranging from 0 to 9.

Geometric distortions are either random or systematic. The former are difficult to correct and typically occur on aircraft buffeted by winds. The best solution is to ‘rubber-stretch’ the image, using landmarks distributed around the imagery that have exact locations (Ground Control Points or GCPs), known by map co-ordinates or GPS readings, onto which the distorted GCP locations on the imagery are stretched. Systematic distortions are relatively easy to correct, the commonest being the ‘parallelogram effect’ produced by the rotation of the Earth in the seconds that it takes an satellite sensor to scan 100-200 km of a given scene.

Sensor noise may be caused by faulty scanner heads or overloading of a given sensor, such as Landsat’s thermal band, often resulting in a line of DN values with values of either 0 or 255. This can be corrected by substituting an erroneous value with the mean value from the pixels above and below it. Most modern imagery has already been pre-processed, removing geometric errors and geo-correcting the imagery to fit regional map projections. For more details, the reader is referred to the textbooks of Lillesand & Kiefer (2000), Drury (2001) and Mather (1999).

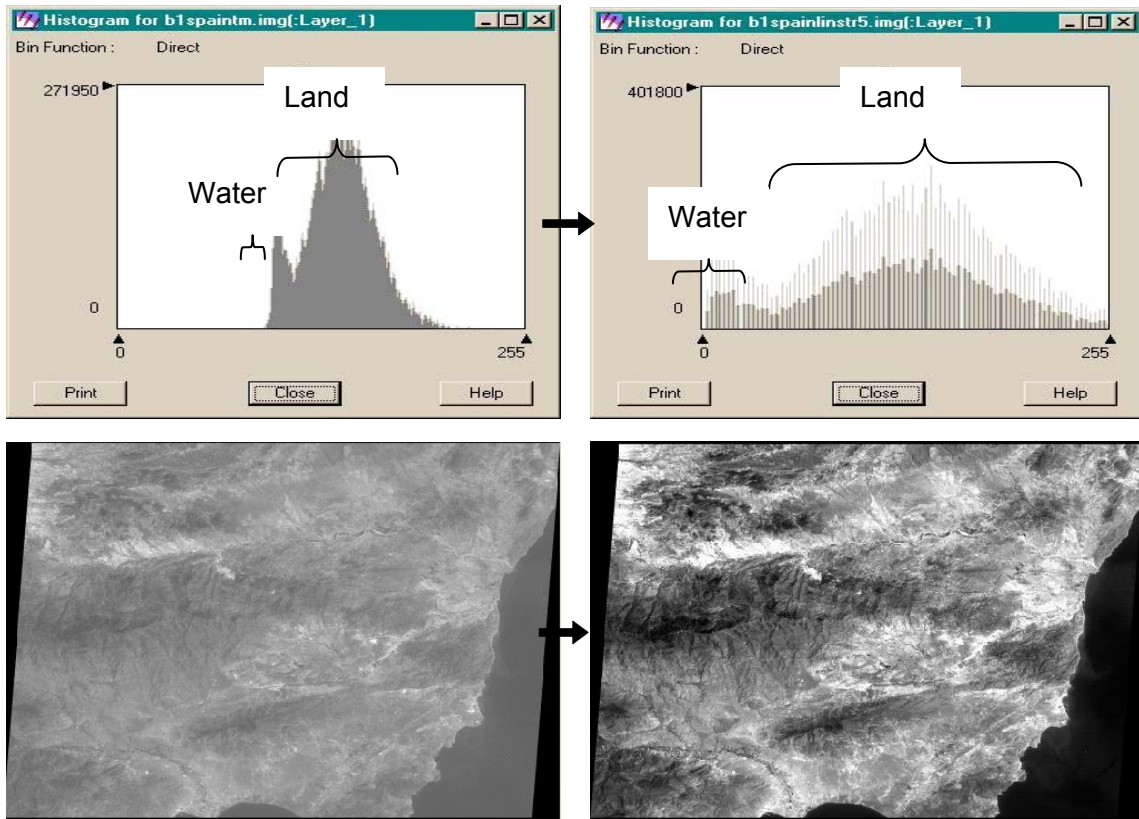
8.5.2 Image Enhancement

There are many ways to enhance digital imagery: contrast stretching, spatial filtering, colour composites, band-ratio images and advanced statistical techniques, such as Principal Components Analysis. The digital imagery used in the following examples is of Almeria province, along the Mediterranean coast of SE Spain.

8.5.3 Contrast stretching

This is a relatively straight-forward way of enhancing differences in the tone and texture of digital imagery. The process is illustrated by the graphs in Land Figure 8-8, each of which is underlain by the corresponding greyscale image. The illustrations on the left are of raw, unprocessed Landsat data: note that (i) the range of DN values in the histogram is narrow, ranging from about 100 to 180, and (ii) the corresponding image is relatively dark. The histogram on the right consists of the same dataset, re-sampled to cover the entire 0-255 range of DN values, resulting in an image with much better contrast. There are many types of contrast stretch: that used in Land Figure 8-8 is the Histogram Equalisation type, but

various types of Linear Stretch can be used to mask or enhance features with distinct DN ranges, such as the low DN ranges associated with water.



Land Figure 8-8 Raw Landsat data (left) and stretched data (right).

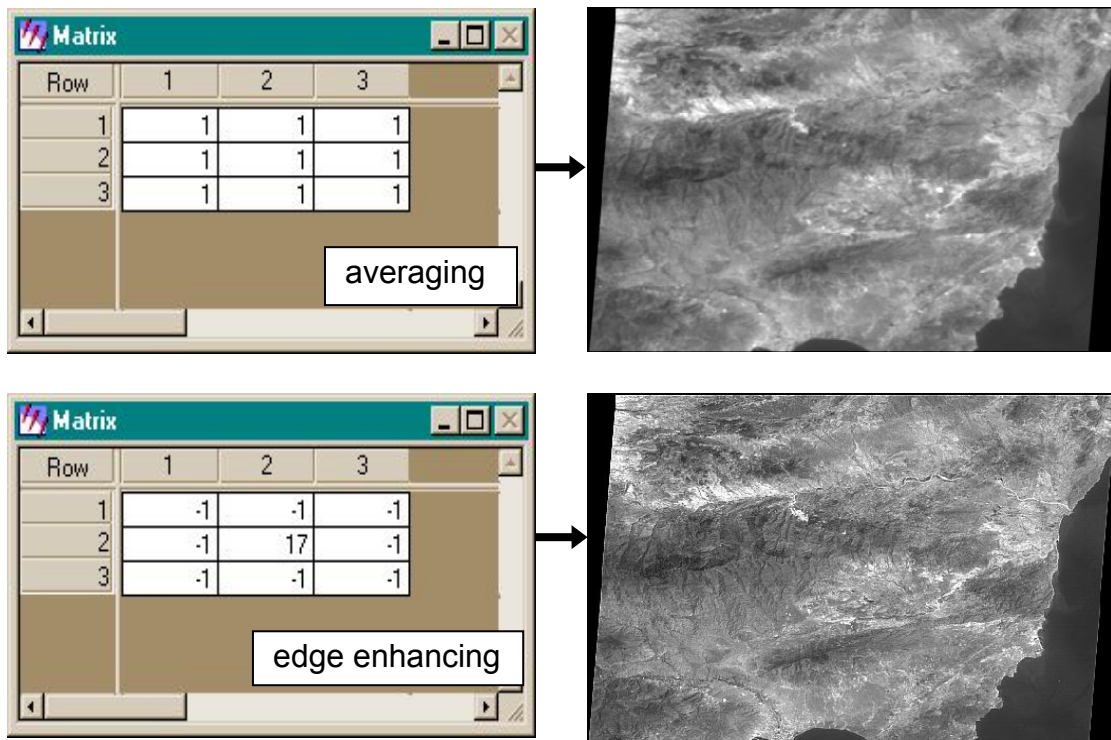


Figure 8-9 Two types of spatial filter (left) and the resulting images (right).

8.5.4 Spatial filtering

A digital image can be modified by moving a spatial filter, or kernel, through the matrix of DN values, rather like using a moving average. The top pair of illustrations in Figure 8-9 shows a smoothing filter and the resulting image (compare with the original contrast stretched image in Land Figure 8-8), in which each pixel has been given the average DN value from all eight adjacent pixels. The lower set of illustrations in Figure 8-9 shows the results of the opposite process, in which differences between adjacent pixels are enhanced, sharpening the image.

8.5.5 Colour composite images

False-colour images are the most widely used product of image processing: the saying goes that “a picture can tell a thousand stories” – even more so if it is in colour. By allocating three of the bands (i.e. wavelengths) from a scanned image to the blue, green and red colour-guns of a computer screen, a false-colour image is produced, as illustrated in Plate 11. A list of composite image band combinations and the resulting highlighted features, using Landsat TM and ETM imagery, is given in Table 8-2 and Table 8-3.

A ‘true colour’ composite image is produced by allocating the R, G, and B colour guns to the R, G and B wavebands of a given set of multi-spectral imagery: using Landsat TM that would correspond to bands 3, 2 and 1, with the resulting image described as ‘RGB321’ in remote sensing short-hand. Creating ‘false colour’ images is very useful, as it allows us to view images captured in parts of the spectrum that would otherwise be invisible to our eyes, such as infra-red or ultra-violet. ‘False Colour Infra-Red’ (FCIR) images are particularly useful, as they allow us to view the pronounced variations in Near Infra-Red (NIR) reflectance associated with photosynthesizing vegetation. Using Landsat TM, FCIR images are created by allocating the R, G and B colour-guns to bands 4 (NIR), 3 (R) and 2 (G) respectively (i.e. RGB432). FCIR images look a bit odd at first, as water (which absorbs NIR radiation) is black, vegetated areas are shades of red and non-vegetated areas are shades of light grey, but an inspection of the composite images in Plate 11 illustrates how relatively subtle variations in vegetation cover are enhanced when using FCIR. Table 8-2 and Table 8-3 below summarise the uses of various colour composite images - using Landsat and ASTER imagery - for detecting variations in types of land cover, soils, rocks and minerals.

Table 8-2 Some useful waveband display combinations for Landsat TM and ETM+ (view as RGB colour images).

R G B	Highlighted Features
3 2 1	'True colour' image
4 3 2	False-colour infra-red: vegetation chlorophyll shows as red
1 3 5 2 4 5 7 3 1	Vegetation and soils
4 5 3 4 5 6 4 5 7	Soils and rock types
5 4 1 5 3 1 7 4 1	Hydrothermal alteration of volcanic rocks
7 5 1	Discrimination between Fe-rich soil and rock
5 3 1 6 7 2 2 3 4 6 5 4	Useful with various vegetation and rock types
6 7 5	Urban/rural boundaries
1 7 4	Coastal sediment plumes and variations in land cover types
7 4 2	Coastal features (- best with linear stretching)

Table 8-3 Some useful waveband ratios for Landsat TM and ETM (best viewed in greyscale)

Band ratios	Highlighted features
4/3	Vegetation Index: responds to green biomass, chlorophyll content and leaf water stress
(4-3) / (4+3)	Normalised Difference Vegetation Index (NDVI): responds to green biomass, chlorophyll content and leaf water stress. NB not suitable for regions with <30% vegetation cover.
5/4	Infrared Index: responds to changes in green biomass and water stress better than NDVI.
5/7	Responds to soil moisture content; gypsum and different types of clay
3/1	Responds to Fe-rich soil or rock
4/5	Separates hydrous rocks from Fe-rich rocks

Table 8-4 ASTER band combinations and their uses in geological mapping. Band ratios are best viewed as greyscale; band composites in RGB colour.

ASTER bands	Highlighted features
468 or 631	Useful for general geological mapping
321	False Colour InfraRed (photo-synthesising vegetation shows as red)
2/1 or ((2/1) 3 1) 4/1 or 4/3	Ferric oxides
5/3 or ((1/2)+(5/3)) 7/4	Ferrous oxides (7/4 applies to ferrous oxides in carbonate or silicate rocks)
456 (4+6) / (5x2) 5/6 7/6 7/5	Hydrothermal (argillic) alteration
4/3 2/1 6/4	Regolith mapping (ferricrete / laterite, saprolite)
(7+9) / (8x2) 13/14 (6+8) / (7x2)	Carbonates (nb. the third combination highlights dolomitised carbonates)
11/10, 13/12 14/12 11/(10+12)	Quartz
13 12 10	Quartz, carbonate & mafic minerals
14 12 10	Quartz, basic minerals & saline soils
12/13	'Basic minerals': garnet, pyroxene, epidote, chlorite

8.5.6 Band ratios

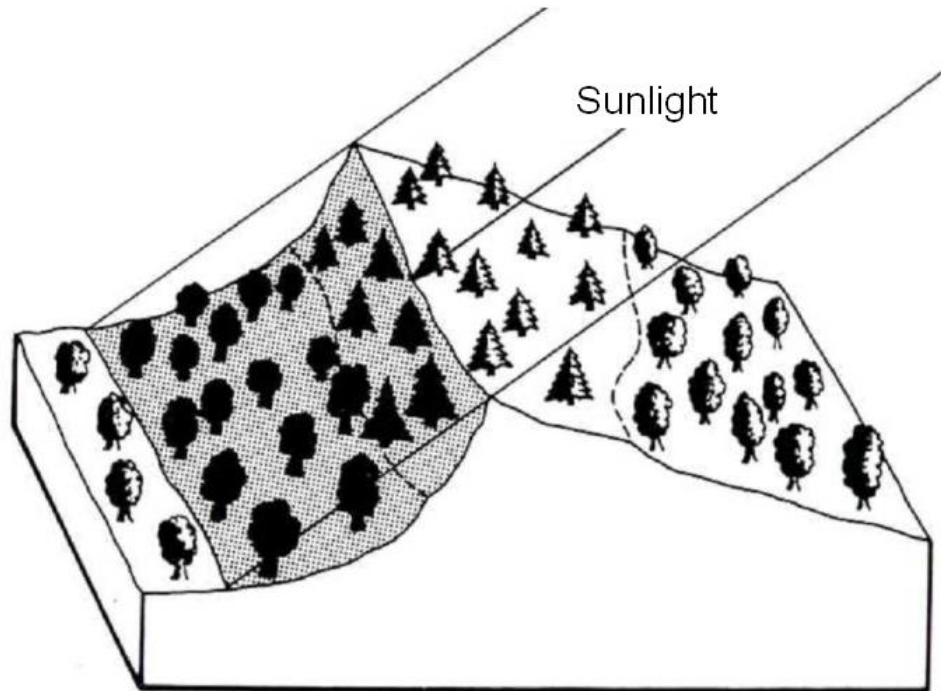
With a given multi-spectral dataset, if you divide all of the DN values in one band by all of the DN values from corresponding pixels in another band, certain features that either strongly absorb or strongly reflect radiation in the two bands will be highlighted. For instance, dividing Landsat TM band 5 by band 3 highlights areas of gypsum-rich soil and certain clay minerals associated with hydrothermal activity in volcanic terrain. Table 8-4 summarises the various types of land cover, rocks and minerals that can be detected using band ratios with Landsat and ASTER imagery. Another useful aspect of band ratio images is that the effects of shadows are eliminated, as illustrated in Figure 8-10. The pronounced difference between the relative levels of red and near infra-red radiation reflected by vegetation can be used to create an index of vegetation abundance, the most widely used example being the Normalised Difference Vegetation Index (NDVI):

$$\text{NDVI} = (\text{NIR} - \text{Red}) / (\text{NIR} + \text{Red})$$

With Landsat TM or ETM+:

$$\text{NDVI} = (\text{Band 4} - \text{Band 3}) / (\text{Band 4} + \text{Band 3})$$

NDVI has been used very effectively with regional weather satellite imagery of Amazonia to quantify and monitor the loss of rainforest since the 1970s. The use of NDVI in semi-arid regions, as in Figure 8-11, should be treated with caution, due to large amounts of bare soil and rock that will influence the reflectance values. Specially modified vegetation indices for use over arid regions have been developed and are reviewed by Lillesand & Kiefer (2000).



Land cover	Illumination	Digital number		
		Band A	Band B	Ratio (A / B)
Deciduous	Sunlit	65	72	0.90
	Shadow	19	21	0.90
Coniferous	Sunlit	32	48	0.67
	Shadow	10	15	0.67

Figure 8-10 Use of band ratio processing to remove the effects of shadow (after Lillesand & Kiefer 2000).

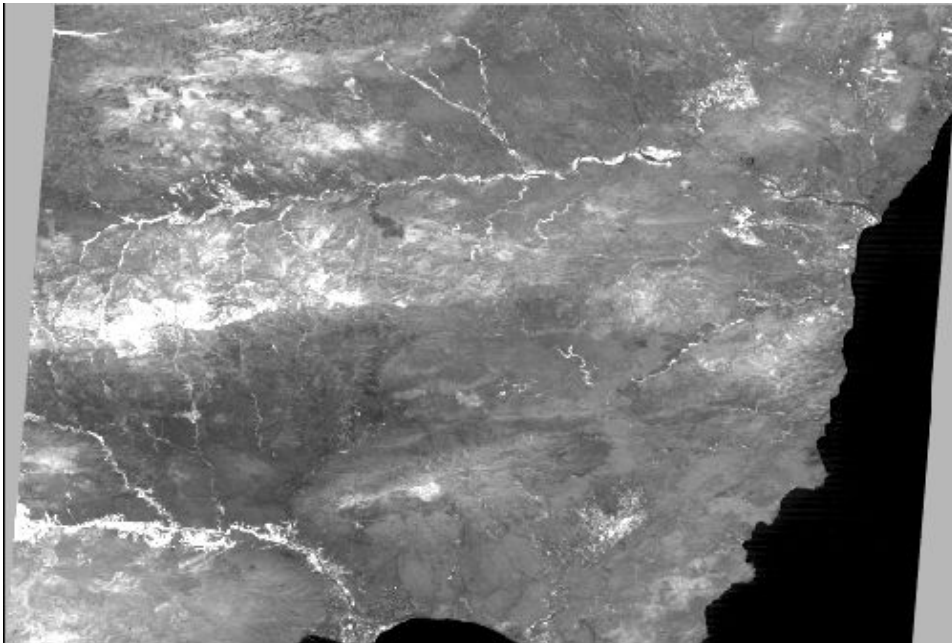


Figure 8-11 NDVI image of Almeria province, SE Spain. Areas with abundant vegetation show as white. This region contains the largest expanses of semi-arid and desert terrain in Europe. Most of the vegetation is limited to river valleys (bottom left and upper half of the image) and the summits of mountain ranges, notably in the top left quarter of the image.

8.5.7 Image classification

The subdivision of Earth surface features into different types on the basis of their spectral responses is known as classification. There are two types of classification: unsupervised and supervised, with the latter being more complicated but also potentially more accurate.

Unsupervised classification is carried out by the image processing software without any initial input, or ‘training’, from the user. The process can be illustrated with reference to Figure 8-12. Diagram A shows four different land cover types, each with a distinct spectral signature. The differing spectral responses can be more effectively distinguished by plotting the DN values from the bands of the original Landsat imagery against each other, as illustrated in Figure 8-12B. This produces distinct clusters of DN values, along with a modified image on which each cluster is colour-coded. The user then has to allocate each cluster to its corresponding land cover type, providing a legend, thereby turning the colour-coded cluster analysis image into a land cover map.

Supervised classification requires the user to select training areas containing about 100 pixels of each land cover type: these pixels are used to ‘teach’ a computer to recognise the spectral responses of each land cover type. A legend for the ensuing land cover map is built up as the user inputs the training areas for each land cover type. The software then uses the training areas to derive statistical summaries of each land cover type’s spectral response, from which it goes on to classify all of the remaining pixels in the image. The purer the sample of pixels in the training area for each land cover type, the better the accuracy of the ensuing classification.

Classification based on a spectral reflectance from a single band and then from two bands is illustrated graphically in Figure 8-12. Including a third band in the classification routine

will improve the discrimination between land cover types, as illustrated in the 3-D graph in Plate 13. Using multispectral or hyperspectral imagery, classification software can utilise n bands in n dimensions, giving increasingly better separations between land cover types – in some cases allowing automated mapping based solely on the varying spectral responses along scan lines. The maths behind image classification can be complex: the reader is referred to Lillesand & Kiefer (2000), Drury (2001), or Mather (1999) for useful summaries

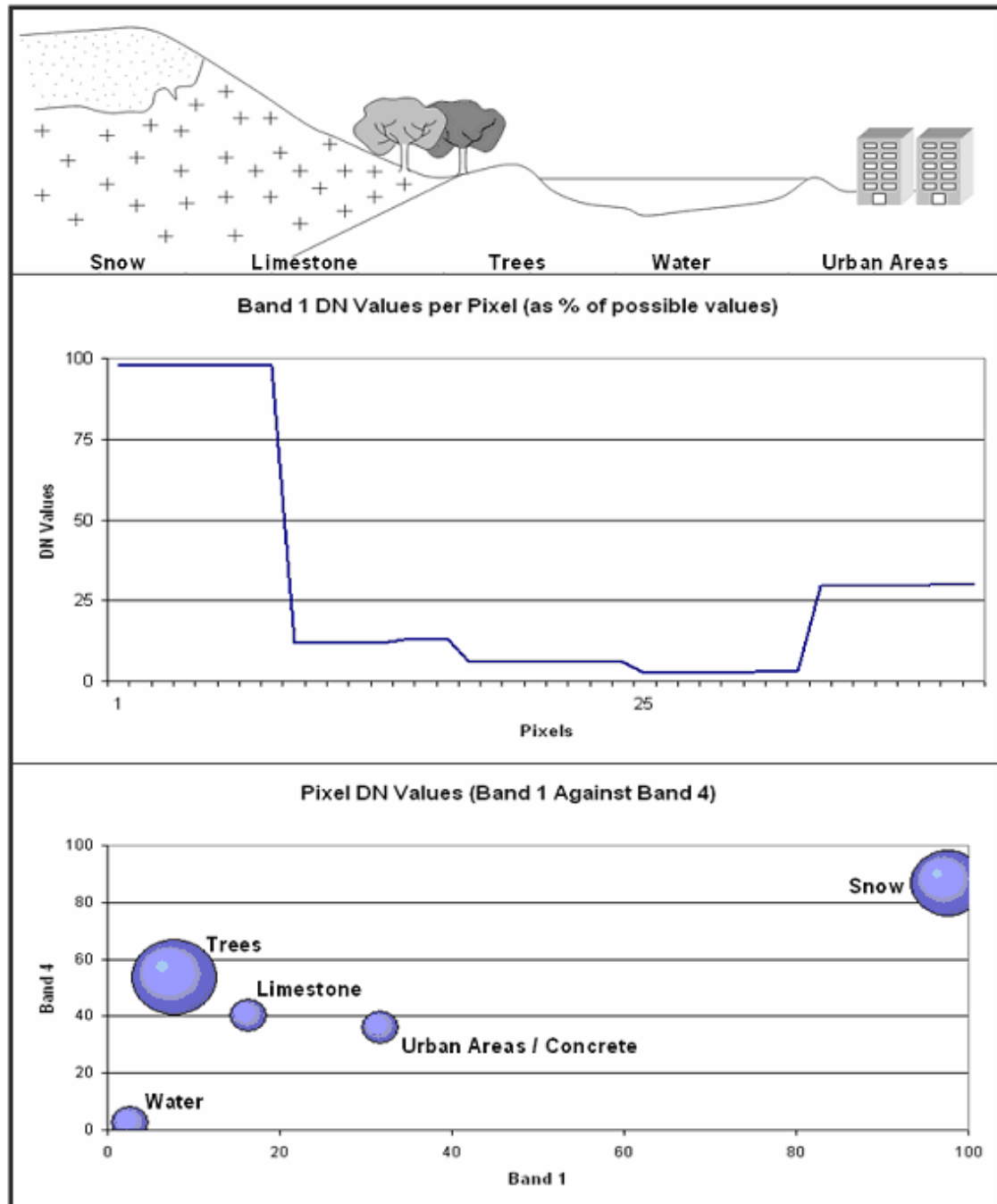


Figure 8-12 Digital image classification, for an idealised landscape (top). Upper graph shows variations in Band 1 reflectance along a scan line: note that the high values for snow and low values for water. The lower graph is a plot of reflectance values for Band 1 against those for Band 4: note the distinct clustering of values for each of the land cover types.

